Inorg. Chem. **1984**, *23*, 2505–2509

Contribution from the Department of Physical Sciences, Mills College, Oakland, California 94613,
and Department of Chemistry, University of Washington, Seattle, Washington 98195

An ab Initio Quadratic Force Field for Methyldiborane

DAVID D. KEEPORTS*† and DAVID F. EGGERS‡

Received December 2, 1983

A quadratic force field for methyldiborane has been determined from ab initio calculations using a 4-21 basis set. A preliminary matching of published infrared and Raman experimental frequencies to calculated frequencies was made after the application of scale factors to the initial ab initio force constants. Additional least-squares refinement of force constants provided a fit of calculated frequencies to 35 experimental frequencies for $B_2H_5CH_3$ and $B_2D_5CH_3$ with a mean difference of 8.9 cm^{-1} or 0.62%. Infrared intensities were calculated and compared to experimental values. Previous vibrational assignments are discussed in light of the frequencies predicted by the ab initio force field. A threefold barrier of 7.37 kJ mol^{-1} was calculated for the methyl torsion of methyldiborane.

Introduction

The effects of methylation upon the structure and vibrational frequencies of the electron-deficient framework of diborane have been considered in numerous previous studies.[1-9] Consistent assignment of fundamental frequencies for methylated diboranes is quite difficult, however, due to considerable spectral complexity. In the case of methyldiborane, both infrared and Raman activities are predicted for all of the molecule's 27 normal modes due to low molecular symmetry. A major source of additional spectral features results from the 20% natural abundance of boron-10 atoms, since 32% of all methyldiborane molecules contain one boron-10 atom and one boron-11 atom and 4% of all molecules contain two boron-10 atoms. Finally, the instability of methyldiborane with respect to disporportionation into diborane and dimethyldiboranes can lead to spectral features due to impurities. While disporportionation can be minimized by the study of samples at low temperatures, additional complications due to correlation field splittings can arise in solid-state spectra.

The present study was undertaken to derive a reliable force field of predictive value in the assignment of methyldiborane fundamentals. Force constants for *cis*- and *trans*-1,2-dimethyldiborane have been reported previously.[4] However, some of the force constants of that study, obtained by least-squares fitting to questionable vibrational assignments, are physically quite unrealistic. An attempt had been made by us to obtain a force field for methyldiborane by least-squares refinement of force constants from previously published force fields for diborane and ethane. Since the number of distinct force constants in the complete force field for methyldiborane (208) is much greater than the number of experimentally available frequencies for the molecule and its deuterated derivatives and since much uncertainty is present in the assignment of fundamentals, the method of least-squares refinement of force constants taken from other molecules was judged highly unreliable and was abandoned. The ab initio method used in the present study was selected due to the success of calculations using similar basis sets in predicting the vibrational frequencies of other molecules, particularly those of diborane.[10]

Method

Initial unrefined force constants were calculated at the University of Texas at Austin by using the ab initio Hartree–Fock gradient program TEXAS.[11] A geometry optimization was followed by the calculation of forces upon all atoms for the molecule in its reference geometry as well as for the molecule following small positive displacements of each of its internal coordinates. The 4-21 basis set used for all calculations as well as details of the method of calculation are described elsewhere.[12]

As a test of the reliability of the 4-21 basis set in the prediction of the properties of molecules with electron-deficient bonds, a geometry optimization using this basis set was first carried out on diborane. The previous ab initio study of Blom and Müller[10] has demonstrated the reliability of a 4-31G basis set in the prediction of both the geometry and vibrational frequences of this molecule. The geometry obtained with the very similar basis set of the present study differed only slightly, as expected, from that obtained in the previous study. Compared to the 4-31G geometry, boron–terminal hydrogen and boron–bridging hydrogen distances were lengthened 0.001 and 0.004 Å, respectively, while H_tBH_t and H_bBH_b angles were changed by +0.45 and −0.55°, respectively.

Geometry optimization was carried out for methyldiborane, with initial estimates of bond lengths and angles taken from microwave data for methyldiborane[8] and electron diffraction data for *cis*- and *trans*-1,2-dimethyldiborane.[5] A correction of +0.005 Å was applied to the optimized carbon–hydrogen and boron–terminal hydrogen bond lengths[12] to obtain the reference geometry used in the calculation of force constants (see Figure 1): $r(B_1B_2) = 1.823$ Å, $r(B_1H_3) = 1.308$ Å, $r(B_2H_3) = 1.347$ Å, $r(B_1H_5) = 1.183$ Å, $r(B_1H_6) = 1.185$ Å, $r(B_2H_7) = 1.187$ Å, $r(B_2C) = 1.584$ Å, $r(CH_9) = 1.089$ Å, $r(CH_{10}) = 1.092$ Å, $\alpha(H_3B_1H_4) = 95.1°$, $\alpha(H_3B_2H_4) = 91.5°$, $\alpha(B_2B_1H_5) = 118.5°$, $\alpha(B_2B_1H_6) = 118.8°$, $\alpha(B_1B_2H_7) = 115.4°$, $\alpha(B_1B_2C) = 121.6°$, $\alpha(B_2CH_9) = 113.4°$, $\alpha(B_2CH_{10}) = 110.3°$, $\alpha\,(H_{10}CH_{11}) = 106.7°$.

The large difference in $r(B_1H_3)$ and $r(B_2H_3)$ indicates that the diborane ring is distorted considerably by the introduction of the methyl group. This ring distortion is not reported in previous microwave structural determinations for methyldiborane.[7,8] Very good agreement is found between the calculated BC distance of 1.584 Å and the BC distances for *trans*-1,2-dimethyldiborane (1.581 Å) and *cis*-1,2-dimethyldiborane (1.579 Å) from electron diffraction measurements.[5] This calculated BC distance lies within the upper limit of the large experimental uncertainty of the microwave value of 1.49 (10) Å reported by Chiu, Burg, and Beaudet.[8] The calculated values of 1.183, 1.185, and 1.187 Å for boron–terminal hydrogen distances are low compared to the microwave values of 1.195 (9), 1.187 (5), and 1.20 (1) Å.[8] From the reference geometry, principal moments of inertia are calculated as 15.73, 74.34, and 83.22 amu Å^2 for $^{11}B_2H_5CH_3$ and

---

(1) Lehmann, W. J.; Wilson, C. O.; Shapiro, I. *J. Chem. Phys.* **1960**, *32*, 1088.
(2) Carpenter, J. H.; Jones, W. J.; Jotham, R. W.; Long, L. H. *Spectrochim. Acta, Part A* **1970**, *26A*, 1199.
(3) Carpenter, J. H.; Jones, W. J.; Jotham, R. W.; Long, L. H. *Spectrochim. Acta, Part A* **1971**, *27A*, 1721.
(4) Kapshtal', V. N.; Sverdlov, L. M. *Russ. J. Phys. Chem.* (*Engl. Transl.*) **1965**, *39*, 1169.
(5) Hedberg, L.; Hedberg, K.; Kohler, D. A.; Ritter, D. M.; Schomaker, V. *J. Am. Chem. Soc.* **1980**, *102*, 3430.
(6) Eggers, D. F.; Kohler, D.; Ritter, D. *Spectrochim. Acta, Part A* **1978**, *34A*, 731.
(7) Penn, R. E.; Buxton, L. W. *J. Chem. Phys.* **1977**, *67*, 831.
(8) Chiu, C. W.; Burg, A. B.; Beaudet, R. A. *Inorg. Chem.* **1982**, *21*, 1204.
(9) Chiu, C. W.; Burg, A. B.; Beaduet, R. A. *J. Chem. Phys.* **1983**, *78*, 3562.
(10) Blom, C. E.; Müller, A. *J. Chem. Phys.* **1978**, *69*, 3397.
(11) Pulay, P. *Theor. Chim. Acta* **1979**, *50*, 299.
(12) Pulay, P.; Fogarasi, G.; Pang, F.; Boggs, J. E. *J. Am. Chem. Soc.* **1979**, *101*, 2550.

† Mills College.
‡ University of Washington.

0020-1669/84/1323-2505$01.50/0

Table I. C_s Symmetry Coordinate Definitions for Methyldiborane[a]

1	$2^{-1/2}(r_{1,3}+r_{1,4})$	10	$2^{-1/2}(\alpha_{3,1,6}+\alpha_{4,1,6})$	18	$2^{-1/2}(r_{1,3}-r_{1,4})$
2	$2^{-1/2}(r_{2,3}+r_{2,4})$	11	$2^{-1/2}(\alpha_{3,2,7}+\alpha_{4,2,7})$	19	$2^{-1/2}(r_{2,3}-r_{2,4})$
3	$r_{1,5}$	12	$2^{-1/2}(\alpha_{3,2,8}+\alpha_{4,2,8})$	20	$2^{-1/2}(\alpha_{3,1,5}-\alpha_{4,1,5})$
4	$r_{1,6}$	13	$3^{-1/2}(r_{8,9}+r_{8,10}+r_{8,11})$	21	$2^{-1/2}(\alpha_{3,1,6}-\alpha_{4,1,6})$
5	$r_{2,7}$	14	$6^{-1/2}(\alpha_{9,8,10}+\alpha_{10,8,11}+\alpha_{11,8,9}-\alpha_{2,8,9}-\alpha_{2,8,10}-\alpha_{2,8,11})$	22	$2^{-1/2}(\alpha_{3,2,7}-\alpha_{4,2,7})$
6	$r_{2,8}$			23	$2^{-1/2}(\alpha_{3,2,8}-\alpha_{4,2,8})$
7	$\tau_{1,3,4,2}$	15	$6^{-1/2}(2r_{8,9}-r_{8,10}-r_{8,11})$	24	$2^{-1/2}(r_{8,10}-r_{8,11})$
8	$2^{-1/2}(\alpha_{3,1,4}+\alpha_{3,2,4})$	16	$6^{-1/2}(2\alpha_{2,8,9}-\alpha_{2,8,10}-\alpha_{2,8,11})$	25	$2^{-1/2}(\alpha_{2,8,10}-\alpha_{2,8,11})$
9	$2^{-1/2}(\alpha_{3,1,5}+\alpha_{4,1,5})$	17	$6^{-1/2}(2\alpha_{10,8,11}-\alpha_{9,8,10}-\alpha_{11,8,9})$	26	$2^{-1/2}(\alpha_{9,8,10}-\alpha_{11,8,9})$
				27	$3^{-1/2}(\tau_{9,8,2,7}+\tau_{10,8,2,4}+\tau_{11,8,2,3})$

[a] Modes: 1–17, a′; 18–27, a″.

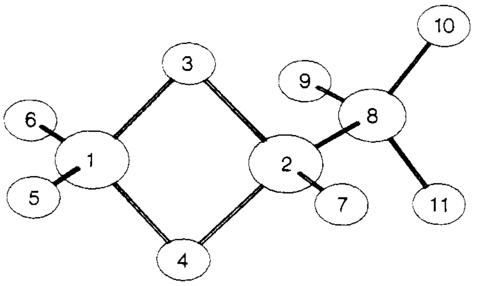

Figure 1. Atomic numbering scheme for methyldiborane.

as 22.97, 85.82, and 98.20 amu Å^2 for $^{11}B_2D_5CH_3$. A dipole moment of 0.594 D is calculated for methyldiborane in its reference geometry. An experimental value of 0.56 D has been reported by Penn and Buxton.[7]

A set of ab initio force constants was determined by the calculation of the forces upon all atoms for the molecule in its reference geometry as well as in geometries resulting from the displacement of each of the molecule's internal coordinates. The set of internal coordinates used included 11 individual bond stretches as well as a set of local symmetry coordinates for bends based upon the symmetry coordinate definitions given by Blom and Müller[10] for diborane and by Blom and Altona[13] for ethane. Displacements of 0.02 Å were used for stretching coordinates, and displacements of 0.02 rad were used for bending coordinates. Factors used to scale the ab initio force constants of diborane[10] and ethane[13] were applied to the diagonal ab initio force constants for methyldiborane; off-diagonal force constants were scaled by the geometric mean of the factors used to scale the corresponding diagonal force constants. The resulting **F** matrix was transformed to the C_s symmetry coordinates defined in Table I, and fundamental frequencies were calculated for $B_2H_5CH_3$ and $B_2D_5CH_3$. Many of the 208 elements of the **F** matrix of methyldiborane were found to be quite small. In order to simplify the force field, off-diagonal elements less than 0.05 were set equal to zero. (Smaller off-diagonal elements for the ring puckering and methyl torsion coordinates were retained, however, due to the small magnitudes of the diagonal force constants associated with these coordinates.) This simplification resulted in the elimination of 116 force constants, with a 0.65% mean change in the calculated frequencies for the two molecules. A preliminary set of infrared intensities was calculated by transforming the dipole derivatives with respect to internal coordinates output by the program TEXAS to dipole derivaties with respect to normal coordinates.

The frequencies calculated from the scaled ab initio force constants generally agreed quite well with the vapor-phase infrared frequencies reported by Lehmann et al.[1] and the liquid Raman frequencies reported by Carpenter et al.[3] Thirty-five experimental frequencies for $B_2H_5CH_3$ and $B_2D_5CH_3$ were assigned to calculated frequencies with a mean difference of 2.1% between experimental and calculated values. The largest discrepancies in assignments occurred in the region of boron–terminal hydrogen stretching, where the six calculated frequencies were on the average 77 cm^{-1} or 3.3% larger than the observed frequencies. Criteria used in frequency assignments included Raman polarization behavior and infrared intensities and band shapes. Infrared bands exhibiting A-type or B-type contours were assigned to modes of a′ symmetry, while bands exhibiting C-type contours were assigned to modes of a″ symmetry. Likewise, polarized Raman lines are expected for modes of a′ symmetry, while depolarized lines are expected for modes of a″ symmetry.

Table II. Scaled and Refined **F** Matrix of Methyldiborane[a]

$F(1,1) = 1.844$
$F(1,2) = 0.060$
$F(1,3) = 0.071$
$F(1,4) = 0.072$
$F(1,6) = -0.098$
$F(1,8) = -0.183$
$F(1,11) = 0.212$
$F(1,12) = 0.252$
$F(2,2) = 1.447$
$F(2,5) = 0.079$
$F(2,6) = 0.202$
$F(2,8) = -0.200$
$F(2,9) = 0.203$
$F(2,10) = 0.209$
$F(3,3) = 3.608$
$F(3,4) = 0.073$
$F(3,10) = -0.092$
$F(4,4) = 3.595$
$F(4,9) = -0.094$
$F(5,5) = 3.465$
$F(5,12) = -0.088$
$F(6,6) = 3.628$
$F(6,8) = -0.092$
$F(6,11) = -0.137$
$F(6,12) = 0.105$
$F(6,13) = 0.086$
$F(6,14) = -0.221$
$F(7,7) = 0.163$
$F(7,9) = 0.083$
$F(7,10) = -0.087$
$F(7,11) = 0.078$
$F(7,12) = -0.133$
$F(8,8) = 1.482$
$F(8,9) = 0.125$
$F(8,10) = 0.117$
$F(8,11) = 0.089$
$F(8,12) = 0.137$
$F(9,9) = 0.877$
$F(9,10) = 0.449$
$F(9,12) = 0.058$
$F(10,10) = 0.941$
$F(10,11) = 0.058$
$F(11,11) = 0.914$
$F(11,12) = 0.487$
$F(11,16) = -0.098$
$F(12,12) = 1.189$
$F(12,15) = -0.074$
$F(12,16) = -0.183$
$F(13,13) = 4.879$
$F(13,14) = 0.129$
$F(14,14) = 0.488$
$F(15,15) = 4.712$
$F(15,16) = 0.144$
$F(15,17) = -0.156$
$F(16,16) = 0.522$
$F(17,17) = 0.578$

$F(18,18) = 1.483$
$F(18,19) = 0.131$
$F(18,20) = 0.177$
$F(18,21) = 0.172$
$F(18,22) = -0.093$
$F(18,23) = -0.095$
$F(18,27) = -0.003$
$F(19,19) = 1.440$
$F(19,20) = -0.092$
$F(19,21) = -0.093$
$F(19,22) = 0.186$
$F(19,23) = 0.179$
$F(19,25) = -0.065$
$F(19,27) = 0.0016$
$F(20,20) = 0.432$
$F(20,21) = 0.095$
$F(20,23) = 0.089$
$F(20,27) = 0.0025$
$F(21,21) = 0.465$
$F(21,22) = 0.086$
$F(21,27) = -0.0033$
$F(22,22) = 0.414$
$F(22,23) = 0.127$
$F(22,27) = 0.001$
$F(23,23) = 0.667$
$F(23,25) = -0.119$
$F(23,27) = 0.010$
$F(24,24) = 4.719$
$F(24,25) = 0.170$
$F(24,26) = 0.164$
$F(24,27) = -0.009$
$F(25,25) = 0.463$
$F(25,27) = 0.0056$
$F(26,26) = 0.539$
$F(26,27) = 0.0097$
$F(27,27) = 0.0167$

[a] Units of mdyn Å^{-1}, mdyn, and mdyn Å for stretching, stretching/bending, and bending force constants, respectively.

A least-squares refinement of force constants was carried out by using computer programs written by Schachtschneider.[14] Diagonal force constants were allowed to vary in groups of two to six during the force constant refinement. No notable further improvement in the agreement of calculated and experimental frequencies was obtained when diagonal force constants were then allowed to vary in larger groups. Calculations diverged when all diagonal force constants within each symmetry block were allowed to vary simultaneously. Due to the lack of reliable low-frequency data, no attempt was made to refine the original scaled diagonal force constant for the methyl torsion. With one exception, the original scaled off-diagonal force constants were not refined. The interaction force constant between the B_1H_5 stretch and the B_1H_6 stretch, originally eliminated due to its small magnitude (0.024), was reintroduced and refined to a value of 0.073. Frequencies calculated from the refined force constants differ from the 35 assigned frequencies by a mean of 8.9 cm^{-1} or 0.62%. It should be emphasized that while the final force field is consistent with both the ab initio calculations and the experimental frequencies, the introduction of the least-squares adjustment of force constants leads to a force field that

---

(13) Blom, C. E.; Altona, C. *Mol. Phys.* **1976**, *31*, 1377.

(14) Schachtschneider, J. H. "Vibrational Analysis of Polyatomic Molecules. V and VI", Technical Reports 231-64 and 57-65; Shell Development Co.: Emeryville, CA.

Table III. Calculated vs. Experimental Frequencies for $B_2H_5CH_3$

mode	calcd freq^a		obsd freq^b				approx description
a′ 1	2952	2.7	2941	IR	3.5		$\nu_a(CH_3)$, in plane
2	2908	0.99	2911	R			CH_3 sym str
3	2596	9.5	2571	IR	21		$\nu_a(BH_2)$
4	2541	7.7	2522	R			$\nu_s(BH_2)$
5	2525	14	2502	R			$\nu(BH)$
6	2105	4.1	2102	R			$\nu(BH')$, sym, in phase/$\nu(BB)$
7	1616	100	1592	IR	100		$\nu(BH')$, asym, in phase
8	1481	0.32	1481	IR	4.8 i		$\delta_a(CH_3)$, in plane
9	1318	3.4	1319	IR	6.5	A	CH_3 sym bend
10	1181	5.1	1164	R			BH_2 sym bend
11	1137	22	~1136	IR	28		BH in-plane bend
12	1055	3.4	1043	R			BH_2 rock/ring pucker/CH_3 rock
13	987	0.23	996	R			CH_3 rock/$\nu(BC)$
14	868	0.42	901	IR	2.6		BH_2 rock/CH_3 rock
15	673	0.29					$\nu(BB)$/CH_3 rock
16	562	0.22	576	R			ring pucker/BC in-plane bend/CH_3 rock
17	221	0.21					ring pucker
a″ 18	2951	2.4	2941	IR	3.5		$\nu_a(CH_3)$, out of plane
19	1794	6.4	1793	IR	1.6		$\nu(BH')$, sym, out of phase
20	1738	0.11					$\nu(BH')$, asym, out of phase
21	1433	0.44	1430	R			$\delta_a(CH_3)$, out of plane
22	1136	0.004	~1136	IR			BH_2 twist/BH out-of-plane bend
23	952	2.5	946	IR	5.1	C	BH_2 wag/BH out-of-plane bend
24	858	0.27					CH_3 wag
25	727	0.15	730	IR	0.1		BH out-of-plane bend
26	477	0.02					BC out-of-plane bend
27	173	0.005					methyl torsion

[a] Calculated frequency in cm^{-1} followed by calculated relative intensity. [b] Observed frequency in cm^{-1} followed by source. IR: from ref 1; frequency followed by relative IR intensity and band type; i = apparent intensity increased by overlap with other bands. R: from ref 3.

Table IV. Calculated vs. Experimental Frequencies for $B_2D_5CH_3$^{a}

mode	calcd frequency		obsd frequency^b			approx description
a′ 1	2952	4.5	2958	7.2		$\nu_a(CH_3)$, in plane
2	2908	1.6	2906^c			CH_3 sym str
3	1948	8.7	1965	18	B	$\nu_a(BD_2)$
4	1871	13	1887	15	A?	$\nu(BD)$
5	1837	15	1855	25		$\nu_s(BD_2)$
6	1496	4.8	1497	2.7		$\nu(BD')$, sym, in phase/$\nu(BB)$/$\delta_a(CH_3)$, in plane
7	1477	0.56				$\delta_a(CH_3)$, in plane
8	1319	3.0	1319	20	A	CH_3 sym bend
9	1172	100	1188	100		$\nu(BD')$, asym, in phase
10	1047	17	1042	20	A	CH_3 rock/$\nu(BC)$
11	979	2.1	976	2.7		CH_3 rock
12	883	6.1	883	11	A	BD_2 sym bend
13	772	1.8				BD_2 rock/ring pucker/BD in-plane bend
14	696	0.02				BD_2 rock/BD in-plane bend
15	636	1.4				CH_3 rock/$\nu(BB)$
16	460	0.09				ring pucker/BC in-plane bend
17	186	0.27				ring pucker
a″ 18	2951	4.1	2958	7.2		$\nu_a(CH_3)$, out of plane
19	1432	0.82	1433	5.6 i	C	$\delta_a(CH_3)$, out of plane
20	1345	7.6				$\nu(BD')$, sym, out of phase
21	1236	0.04				$\nu(BD')$, asym, out of phase
22	911	1.1				CH_3 wag
23	763	1.0				BD_2 twist
24	695	0.58	696	2.3	C	BD_2 wag
25	565	0.28				BD out-of-plane bend
26	389	0.01				BC out-of-plane bend
27	170	0.009				methyl torsion

[a] See Table III for explanations of notations. [b] From ref 1 unless otherwise noted. [c] Reference 17.

is not unique. The final refined force field for methyldiborane in C_s symmetry coordinates is given in Table II. Infrared intensities were recalculated for the normal modes found from the refined force constants. These intensities are presented in Tables III and IV.

Discussion

Good agreement is seen in general between the refined methyldiborane force constants in Table II and the corresponding scaled ab initio force constants for diborane[10] and ethane.[13] When the **F** matrix for diborane is transformed into internal coordinates involving individual bond stretches, the diagonal force constants for boron–terminal hydrogen stretching and boron–bridge hydrogen stretching are 3.646 and 1.736, respectively. The refined diagonal force constants of 3.608, 3.595, and 3.465 for the stretching coordinates of methyldiborane involving H_5, H_6, and H_7 indicate a weakening of bonds between the boron atoms and the terminal hydrogen atoms for this molecule relative to the corresponding bonds for diborane. This bond weakening is consistent with the approximately 30-cm^{-1} decrease in the mean of the observed methyldiborane terminal hydrogen stretching frequencies relative to the mean of the observed diborane terminal hydrogen stretching frequencies. It is found by combining the refined symmetry force constants for boron–bridging hydrogen stretches that the respective diagonal force constants for the B_1H_3 and B_2H_3 stretches are 1.664 and 1.444. This disparity in force constants involving individual boron–bridging hydrogen bond stretches is consistent with the considerable calculated ring distortion in methyldiborane. The respective unscaled ab initio force constants for the B_1H_5, B_1H_6, B_2H_7, B_1H_3, and B_2H_3 stretches are 3.988, 3.955, 3.905, 1.850, and 1.457. Comparison of final refined force constants to initial unscaled ab initio force constants indicates that 0.90 is an appropriate scale factor for diagonal ab initio boron–terminal hydrogen stretching force constants, while no single scale factor applies to both distinct boron–bridging hydrogen diagonal stretching force constants. Comparison of the diagonal BC stretching force constant of methyldiborane (3.628) to the diagonal CC stretching force constant of ethane (4.312)[13] shows magnitudes consistent with the greater calculated length of the former bond (1.584 vs. 1.53 Å).

The scaled diagonal force constant for the methyl torsion of methyldiborane (0.0167) is larger than those calculated for ethane (0.0087) and propane (0.0104).[13] An ab initio determination of the barrier to methyl torsion was carried out by performing a geometry optimization, with the methyl group eclipsed with respect to H_3, H_4, and H_7, and by comparing the energy of this configuration to that of the molecule in its reference geometry. A barrier of 7.37 kJ mol^{-1} was obtained. Comparable barriers to methyl torsion have been reported previously for substituted diboranes. Chiu, Burg, and Beaudet[8] have reported a barrier of 10.5 kJ mol^{-1} for methyldiborane on the basis of microwave measurements. A barrier height of approximately 8 kJ mol^{-1} for the methyl torsion in *trans*-1,2-dimethyldiborane has been reported from an electron diffraction study,[5] while a value of 10.9 kJ mol^{-1} has been reported from a solid Raman study.[6] A microwave value of 5.82 kJ mol^{-1} for the barrier to methyl torsion in 1,1-dimethyldiborane has been recently published.[9] In light of the ab initio barrier height and the experimental values stated here, we concur with the conclusion of Chiu, Burg, and Beaudet[8] that the value of 17.9 kJ mol^{-1} for the torsional barrier in methyldiborane obtained by Penn and Buxton[7] from microwave data is unreasonably large.

On the basis of the method outlined by Fateley and Miller,[15] the tables provided by Herschbach,[16] and the ab initio torsional barrier, the frequency of the methyl torsional mode in $B_2H_5CH_3$ was calculated with the assumption of a cosinusoidal potential function for the torsion. The resulting value of 172.4 cm^{-1} agrees remarkably well with the 173.1-cm^{-1} value for ν_{27} calculated with the assumption of a quadratic potential function.

The assignment of $B_2H_5CH_3$ fundamentals based upon the force field calculated here (Tables III and IV) agrees fairly well with the assignments of Carpenter et al. based upon their Raman spectra and upon the infrared spectra of Lehmann et al. Some differences must be noted, however. Carpenter assigns an infrared feature at 1424 cm^{-1} to ν_8 (a′). Since this feature is the infrared counterpart of the depolarized liquid Raman line at 1430 cm^{-1}, the infrared feature at 1481 cm^{-1} is instead assigned here to ν_8. Carpenter assigns a strong depolarized Raman line at 1043 cm^{-1} to ν_{22} (a″). For several reasons this line is assigned here to ν_{12} (a′). Preliminary measurements by other workers[17] indicate that this feature may be very weakly polarized in the liquid Raman spectrum. Frequency calculations using scaled ab initio force constants prior to least-squares refinement yielded a frequency of 1079 cm^{-1} in the a′ symmetry block and no calculated frequencies between 962 and 1131 cm^{-1} in the a″ symmetry block. Furthermore, Lehmann et al. report an A-type band in the infrared spectrum of $B_2D_5CH_3$ at 1042 cm^{-1}. Normal-mode calculations based upon the refined force field indicate a strong methyl rocking contribution to modes calculated near 1050 cm^{-1} for both $B_2H_5CH_3$ and $B_2D_5CH_3$. On the basis of preliminary frequency calculations, the infrared feature at 901 cm^{-1} assigned by Carpenter to the a″ mode ν_{24} is assigned in this study to the a′ mode ν_{14}. Carpenter's assignment of 638 cm^{-1} to ν_{15} is based upon the assumption of Fermi resonance involving a fundamental near 290 cm^{-1}. The force field of the present study predicts no fundamental near the required frequency. Thus, ν_{15} is left unassigned here. The polarized Raman line at 576 cm^{-1} is assigned here to ν_{16} on the basis of good agreement between measured and calculated frequencies. No fundamentals are calculated near 1900 cm^{-1}. Thus, the infrared band at 1919 cm^{-1} assigned by Carpenter to ν_{19} is assigned here to an overtone or combination. A calculated a″ frequency of 1738 cm^{-1} may be matched with a depolarized liquid Raman feature seen by other workers[17] at 1685 cm^{-1}, while the broad, intense infrared feature from 1130 to 1143 cm^{-1} may mask the a″ mode ν_{22} calculated at 1136 cm^{-1}.

Good order of magnitude agreement is seen between calculated and observed infrared intensities (Tables III and IV). In some cases, calculated intensities may assist in making otherwise difficult assignments. The large observed infrared intensity relative to the calculated intensity (20 vs. 3) for the a′ mode ν_8 of $B_2D_5CH_3$ suggests that the band observed at 1319 cm^{-1} may contain intensity contributions both from ν_8 and from ν_{20} with a calculated frequency of 1345 cm^{-1} and a moderately large calculated intensity. Likewise, the large observed relative intensity (25) of the infrared band of $B_2H_5CH_3$ at 2513 cm^{-1} reported by Lehmann et al.[1] can be explained by the fact that it contains intensity contributions from fundamentals with calculated relative intensities of 7.7 and 14 at calculated frequencies of 2541 and 2525 cm^{-1}.

Approximate normal-mode descriptions are given in Table III for $B_2H_5CH_3$ and in Table IV for $B_2D_5CH_3$. The names given to the stretching modes of the boron–bridging hydrogen bonds are taken from the paper of Lehmann et al.,[1] while the names given to the bending modes involving terminal hydrogens are taken from the paper of Blom and Müller.[10] It is seen that many normal modes contain strong contributions from several different internal motions. It is in some cases impossible to assign a unique frequency to a given internal motion. No normal mode in either molecule can be identified as being predominantly a BC stretch. For both molecules, strong BB stretching contributions are seen in two a′ modes of very different frequencies. Substantial methyl rocking contributions are calculated for fundamentals ν_{12} through ν_{16} of $B_2H_5CH_3$. Particularly interesting is the ring puckering motion. This motion contributes strongly to three a′ normal modes for each molecule. Since the restoring force associated with the puckering motion is small, puckering is readily activated by other motions such as CH_3 rocking, BH_2 wagging, and BC in-plane bending.

In summary, very good agreement has been obtained between experimental frequencies for methyldiborane and frequencies calculated from scaled and refined 4-21 ab initio force constants. Calculated frequencies and intensities have proved

---

(15) Fateley, W. G.; Miller, F. A. *Spectrochim. Acta* **1961**, *17*, 857.

(16) Hershbach, D. R. *J. Chem. Phys.* **1959**, *31*, 91.

(17) Ritter, D. M.; Mikelsons, M. V., private communication.

to be of great value in the clarification of fundamental assignments in the rather complex spectra of a molecule of moderate size and low symmetry. Further vibrational studies of methyldiborane are recommended to identify some low-frequency fundamentals that are presently unassigned but are predicted by the force field presented here.

Acknowledgment. D.D.K. expresses his gratitude to Professor James Boggs for his hospitality and assistance provided during a stay at the University of Texas. This work has been supported by a grant from the Robert A. Welch Foundation. Travel expenses for D.D.K. were provided by a grant from the Mellon Foundation.

Contribution from the Department of Industrial Chemistry, Faculty of Engineering,
Yamaguchi University, Ube 755, Japan

Preparation and Hydriding Behavior of Magnesium Metal Clusters Formed in Low-Temperature Cocondensation: Application of Magnesium for Hydrogen Storage

H. IMAMURA,* T. NOBUNAGA, M. KAWAHIGASHI, and S. TSUCHIYA

Received October 11, 1983

Magnesium metal clusters formed in low-temperature matrices were investigated with a view to forming the metal hydride. In practice, magnesium readily absorbed large amounts of hydrogen under more moderate conditions (P_{H_2} = 460 torr, T = 200–250 °C) when it had been transformed into tetrahydrofuran- (THF-) solvated small particles formed by the cocondensation reaction of magnesium atoms with THF molecules at −196 °C. To elucidate the characteristics of hydrogen sorption of Mg–THF, a comparative study with pure magnesium powder was carried out. It is believed from the H_2–D_2 isotope scrambling measurements that the high activity of the present Mg–THF system for hydrogen absorption is due to a rapid surface process in comparison with the case of the pure magnesium. This identification is reinforced by the employment of surface modification techniques.

Introduction

Hydrogen is a very versatile fuel. It can replace petroleum products as a fuel in almost all, if not all, uses. However, there is a containment problem with regard to obtaining a high energy density. Recently, a great deal of attention has been devoted to metal hydrides as a means of containing hydrogen safely and efficiently. It is known that magnesium can react with hydrogen to form the hydride to an extent exceeding the capacity of liquid hydrogen by up to a factor of 1.6 on a per unit volume basis, which satisfies a practical energy density. This property arouses considerable interest in its application for hydrogen storage. In practice, however, some improvement of hydrogen sorption properties is often required. The changes in the sorption properties of magnesium have been investigated by alloying with other metals[1–6] or plating nickel,[7] because magnesium itself is poor as a hydrogen host due to the slow kinetics of hydriding and dehydriding.

We have recently found[8] that magnesium metal clusters, which have been formed by the reaction of metal atoms with organic media in low-temperature matrices, are able to absorb hydrogen readily under mild conditions and, moreover, without the "activation treatment" consisting of repeated cycles of evacuating, heating to ca. 400 °C, and then pressurizing at 70–200 atm of hydrogen. In organic chemistry this low-temperature codeposition method has been known to afford very effective reagents in which the active metal particles are utilized in slurry form.[9]

Studies of the changes in the properties of hydrogen sorption are of fundamental interest. Accordintly, to establish the nature of the magnesium formed by clustering of metal atoms in tetrahydrofuran (THF) vapor, the characteristics of hydrogen sorption were examined in comparison with the results obtained by using pure magnesium activated by the conventional method.

Experimental Section

The active magnesium metal clusters were prepared from the best grade (>99.95%) of elemental magnesium obtainable commercially (Furukawa Magnesium Co. Ltd.). Tetrahydrofuran (THF), which was reagent grade, was thoroughly dehydrated by sodium wire before cocondensing with the high-temperature magnesium species. The apparatus used to prepare the Mg–THF matrix was a reaction vessel containing a THF inlet system and fitted with a heating part consisting of a spiral-shaped tungsten filament (o.d. = 1 mm; The Japan Lamp Industrial Co. Ltd.) connected between tungsten rod electrodes (2.0 × 500).

In a standard procedure for the preparation of Mg–THF the reaction zone was evacuated to a pressure of ca. 10^{-6} torr and then cooled with liquid nitrogen (−196 °C). The tungsten wire heater was gradually energized to vaporize magnesium atoms, and simultaneously the inlet needle valve was slowly opened to introduce THF vapor (ca. 10^{-2} torr) into the system. During the vaporization of 1 g of magnesium, about 5 mL of THF was codeposited on the inner cooled surface of the reactor over a period of 15 min. After completion of the reaction, a dark gray matrix was present and the vessel was allowed to warm to room temperature under vacuum. The excess THF was pumped off, leaving a dry active Mg–THF powder.

The activated magnesium in the form of a fine powder was produced by repeated procedures of hydrogenation at 80 atm and dehydrogenation at 400 °C under vacuum.

Hydrogen absorption measurements were made by using conventional volumetric equipment. Prior to every run the sample was outgassed at 200 °C to ca. 10^{-5} torr for 2 h and then exposed to hydrogen at pressures of up to ca. 460 torr at the prescribed temperatures. The quantity of hydrogen absorbed was calculated from

---

[1] Reilly, J. J.; Wiswall, R. H., Jr. *Inorg. Chem.* **1967**, *6*, 2220.

[2] Reilly, J. J.; Wiswall, R. H., Jr. *Inorg. Chem.* **1968**, *7*, 2254.

[3] Darriet, B.; Pezat, M.; Hbika, A,; Hagenmuller, P. *Int. J. Hydrogen Energy* **1980**, *5*, 173.

[4] Mintz, M. H.; Malkiely, S.; Gavra, Z.; Hadari, Z. *J. Inorg. Nucl. Chem.* **1978**, *40*, 1949.

[5] Douglass D. L. In "Hydrides for Energy Storage"; Andresen, A. F., Maeland, A. J., Eds.; Pergamon Press: Oxford, 1978; p 151.

[6] Akiba, E.; Nomura, K.; Ono. S.; Mizuno, Y. *J. Less-Common Met.* **1983**, *89*, 145.

[7] Eisenberg, F. G.; Zagnoli, D. A.; Sheridan J. J., III. *J. Less-Common Met.* **1980**, *74*, 323.

[8] Imamura, H.; Kawahigashi, M.; Tsuchiya, S. *J. Less-Common Met.* **1983**, *95*, 157.

[9] E.g.: Timms, P. L. *Adv. Inorg. Chem. Radiochem.* **1972**, *14*, 121. Klabunde, K. J.; Efner, H. F.; Satek, L.; Donley, W. *J. Organomet. Chem.* **1974**, *71*, 309. Klabunde, K. J.; Murdock, T. O. *J. Org. Chem.* **1979**, *44*, 3901.